Volume Title
ASP Conference Series, Vol. **Volume Number**
Author

The ALMA view of evolved stars

M. Maercker[1]

[1]*Onsala Space Observatory, Dept. of Radio and Space Science, Chalmers University of Technology, SE-43992 Onsala, Sweden*

Abstract. The Atacama Large Millimeter/submillimeter Array (ALMA) is the largest telescope of its kind, providing the astronomical community with high-spatial resolution, high-sensitivity images between 84 GHz and 720 GHz. During planning and construction of the array, the observatory promised to open a new window on how we observe and investigate the universe around us, and the expectations on how ALMA would affect our understanding of evolved stars were high. ALMA started operations in October 2011, and already with the first observations of an AGB star during Cycle 0, ALMA gave us a unique view of the circumstellar environment around the carbon star R Scl. I review the capabilities of ALMA during the current early science operations and the specifications for full science, and the implications these have for research on evolved stars.

1. Introduction

Observations of molecular emission lines and continuum observations at millimetre and submillimetre wavelengths are one of the main diagnostics for determining the properties of evolved stars. Molecular line emission traces the physical (e.g., size, structure, and temperature) and dynamical properties of the molecular gas in the winds of asymptotic giant branch (AGB) stars and red supergiants. CO is one of the most abundant molecules in the envelopes of evolved stars, and is excited throughout the entire envelope. Therefore CO emission lines are typically used to constrain the mass-loss rates from AGB stars, as well as the envelope size and structure (e.g., Schöier et al. 2002; González Delgado et al. 2003a; Ramstedt et al. 2008; De Beck et al. 2010; Khouri et al. 2014a). Emission from other molecules is used to probe the inner regions of the wind, both in terms of dynamics and chemical processes (e.g., González Delgado et al. 2003a; Schöier et al. 2007; Maercker et al. 2008, 2009; Decin et al. 2010; De Beck et al. 2012; Justtanont et al. 2012; Khouri et al. 2014b, as well as the contribution by T. Khouri in these proceedings). These observations constrain not only the formation of dust particles and hence the mass-loss mechanism, but also the chemical evolution of the star and the yields of elements from evolved stars to the interstellar medium.

Continuum observations at submm-/mm wavelengths probe the dust content in the circumstellar environment around evolved stars through thermal dust emission, as well as the conditions in the extended atmospheres through free-free emission. In particular, the combination of long wavelength observations with data of thermal dust emission at shorter wavelengths is required to constrain dust masses and dust grain properties (Maercker et al., in prep.).

Observations at these wavelengths are most commonly carried out using single-dish telescopes, e.g. the Atacama Pathfinder Experiment (APEX) in Chile, the IRAM 30m telescope in Spain, the OSO 20m telescope in Sweden, or the James Clerk Maxwell Telescope (JCMT) on Hawaii. With telescopes of 12 – 30 m in size, the spatial resolution is typically several tens of arcseconds – very low considering the largest AGB star on the sky, R Doradus, has an angular size of $0\farcs057$ (Richichi et al. 2005). Observations with current interferometers like the IRAM Plateau de Bure interferometer (PdBI) or the Submillimeter Array (SMA) are still limited in angular resolution (typically a few arcseconds). At the same time, the limited number of antennas requires long observing times in order to get sufficient uv-coverage (e.g., Castro-Carrizo et al. 2010; De Beck et al. 2013). For the Northern Hemisphere this will be improved by the upgrade of the PdBI to the NOEMA telescope with baselines of up to 2 km and subarcsecond resolution. However, sensitive, high-resolution images of thermal line emission and continuum emission at millimetre and submillimetre wavelengths have so far not been readily available.

2. The Atacama Large Millimeter/submillimeter Array – ALMA

The Atacama Large Millimeter/submillimeter Array (ALMA) is an interferometer located at an altitude of ≈5000 m on the Chajnantor plateau in the Atacama dessert in northern Chile. The high altitude and extremely dry conditions make the site an ideal place to observe at millimetre and submillimetre wavelengths. When fully completed, ALMA will consist of the main array with 50 12-m antennas, the ALMA Compact Array (ACA) with twelve 7-m antennas, and the total power (TP) array of four 12-m single-dish antennas. It will cover 8 frequency bands in the atmospheric windows between 84 and 950 GHz. The main array will reach baselines of up to 16 km, giving a spatial resolution of $0\farcs012$ at 300 GHz. The ACA and TP arrays will fill in the short- and zero-spacing observations, hence sampling all spatial scales from the highest resolution to very extended emission throughout the field of view (corresponding to the field of view of one array element). The collecting area in the main array will correspond to a surface area of 5655 m^2. With 1225 baselines in the main array, ALMA will efficiently cover the uv-plane, allowing to image the data even in short observations, and making ALMA an effective snapshot instrument. ALMA will have full polarisation capabilities. The correlator already allows for an extremely flexible spectral setup, combining high-resolution spectral windows for spectral line observations with low-resolution windows for continuum observations. More information on ALMA and its capabilities can be found at *www.almascience.org*.

ALMA began early science operations in Cycle 0 in October 2011. At the time the array consisted of 16 12-m antennas in the main array. Two configurations were offered, with maximum baselines of 160 m and 250 m, respectively. Four of the receiver bands were available (bands 3, 6, 7, and 9 at ≈100 GHz, 230 GHz, 300 GHz, and 650 GHz). Depending on the frequency, the spatial resolution was $0\farcs7-5\farcs6$ in the compact configuration, and $0\farcs4 - 3\farcs6$ in the extended configuration. Already at this stage ALMA was the most powerful observing facility of its kind in the world.

In Cycles 1 and 2 (beginning in January 2013 and June 2014, respectively) the number of antennas in the main array was increased to at least 33. Additionally observations with the ACA and TP arrays were offered. While the spectral setup was still relatively restricted in Cycle 0, in Cycles 1 and 2 an extremely flexible setup with vari-

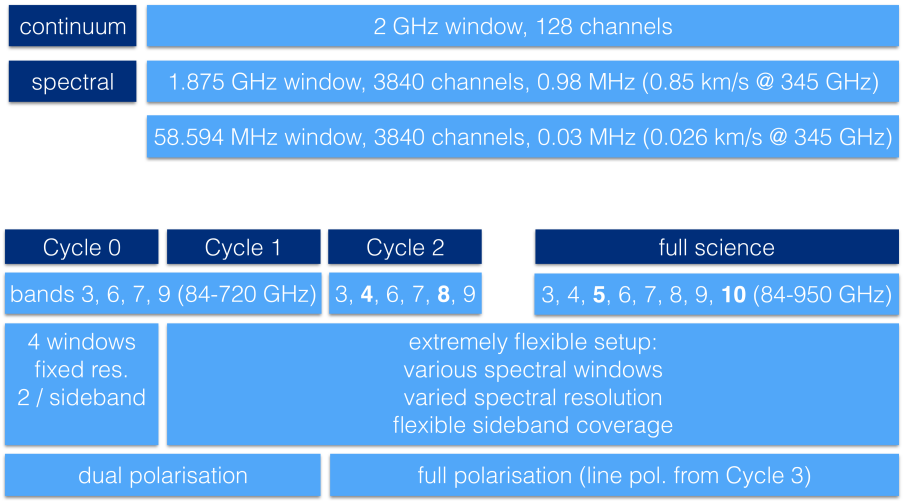

Figure 1. An overview of the ALMA correlator setup capabilities during Early Science cycles compared to full science (Source: *www.almascience.org*).

ous spectral windows with varying spectral resolution and a flexible sideband coverage was offered. In Cycle 2, additionally bands 4 (at 130 Ghz) and 8 (at 450 Ghz) were offered. Cycle 2 observations will end in October 2015, with a deadline for Cycle 3 proposals in the first half of 2015. Figures 1 and 2 show the development of ALMA capabilities in the first 3 cycles compared to full science operations.

2.1. ALMA's contribution to evolved stars

ALMA promises to provide a completely new view on AGB stars and red supergiants, and their circumstellar environments. On average ≈10% of all accepted ALMA proposals belong to stellar evolution. The observations will provide information on the properties of the molecular gas and circumstellar dust, effectively constraining the dynamics and chemistry in evolved stars. They will challenge current models and theories of late stellar evolution, and help determine the contribution of evolved stars to the evolution of galaxies. In particular, ALMA will contribute to evolved star research by greatly improving the sensitivity and spatial resolution of observations, and by offering full polarisation capabilities.

2.1.1. Sensitivity

When operating at full capability, ALMA will have a total collecting area that is equivalent to an 84 m telescope. Cernicharo et al. (2013) observed the carbon AGB star IRC+10216 during Cycle 0 with 16 antennas in one pointing centred on the star. The total on-source integration time was 1 hour. Comparing the observations to 2.5 – 3 hour on-source integrations in the same frequency range using the IRAM 30m telescope, they detect a large number of unidentified lines with ALMA that lie below the sensitivity limit of the IRAM observations (see their Figure 1 for a direct comparison of the ALMA and IRAM spectra).

Figure 2. Examples of the possible resolution at 300 GHz of the ALMA main array during Early Science cycles compared to full science (Source: *www.almascience.org*).

2.1.2. Spatial resolution

The longest ALMA baselines will give a spatial resolution of only a few milliarcseconds. For stars at a few hundred parsec this corresponds to a size of a few stellar radii. ALMA will hence be able to image the dust-formation and wind-acceleration zones of evolved stars. At the same time the high spatial resolution will allow direct comparison to observations of the circumstellar dust at optical wavelengths with, e.g., the *Hubble Space Telescope (HST)*. The power of this was demonstrated in the case of the detached shell around the carbon AGB star R Sculptoris. A comparison between ALMA Cycle 0 observations of CO(3−2) emission in band 7 from the gaseous detached shell (Maercker et al. 2012) and optical observations of stellar light scattered by dust in the dusty detached shell show a direct correspondence of the dust and gas in the shell (Fig. 3). The study of the molecular gas and dust implies a common evolution of these components, constraining the mass-loss properties from AGB stars (Maercker et al. 2014).

2.1.3. Polarisation

In addition to the superior sensitivity and spatial resolution, ALMA provides full polarisation capabilities. In full science ALMA will provide polarimetry for both line and continuum observations. ALMA will be able to detect polarisation in 5 minutes similar to a detection with the SMA in 8 hours. It will thus be able to measure the magnetic field, grain sizes, and the grain alignment around evolved stars and their circumstellar environment in unprecedented detail.

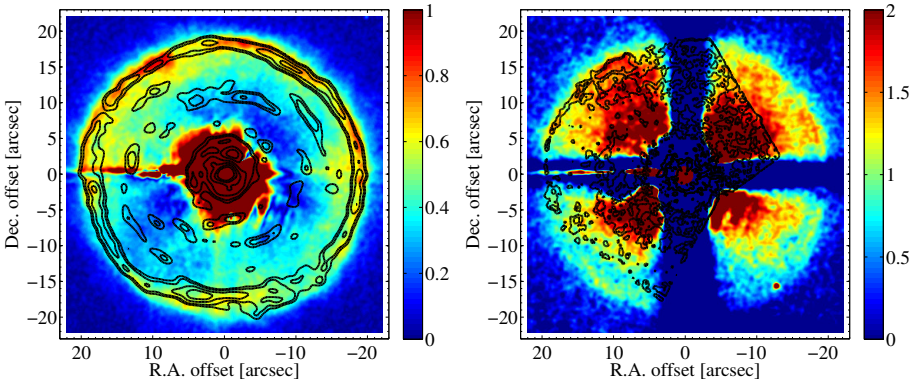

Figure 3. Comparison between dust-scattered stellar light images from PolCor and ALMA and HST data towards the carbon AGB star R Sculptoris. *Left:* ALMA CO(3 − 2) observations at the systemic velocity (contours) overlaid on polarised, dust-scattered stellar light observed with the PolCor instrument on the ESO 3.6m telescope in the R-band. *Right:* HST data taken at 0.8 μm (contours) overlaid on the total intensity images observed with PolCor. in the R-band The comparison shows the close correlation between the molecular emission in the ALMA data with the dust-scattered stellar light images from PolCor and the HST. From Maercker et al. (2014).

3. Early science examples

Already in Early Science ALMA has produced spectacular results in the field of evolved-star research. A few examples illuminating the capabilities of ALMA are given below. A full list of publications based on ALMA observations can be found at *telbib.eso.org*.

3.1. The detached shell around R Sculptoris

The first evolved star to be observed during regular science operations in ALMA Cycle 0 was the carbon AGB star R Sculptoris (Maercker et al. 2012). The observations were taken with 16 antennas in the main array in its Cycle 0 compact configuration, resulting in a maximum spatial resolution of ≈1.2". The total observing time was 6 hours, resulting in an rms noise of 44 mJy/beam at a velocity resolution of 0.5 km/s.

The observations were aimed at imaging the detached shell around R Scl at high spatial resolution in the CO(1 − 0), (2 − 1), and (3 − 2) transitions to effectively constrain the mass, temperature, and physical structure of the shell. The shell was created by the increase in mass-loss rate and expansion velocity during the most recent thermal pulse (e.g., González Delgado et al. 2001, 2003b; Olofsson et al. 2010). However, in addition to the detached shell, the data also show a clear spiral structure extending from the shell inwards to the present-day mass-loss (see Fig. 4, left, Maercker et al. 2012). The spiral is a clear signature of interaction between the AGB wind with a previously unknown binary companion. The spacing between spiral windings depends on the expansion velocity of the wind, and the intensity along the spiral depends on the mass-loss rate from R Scl. Therefore the observations allowed to constrain the evolution of the mass-loss rate since the last thermal pulse observationally for the very first time (Fig. 4, right).

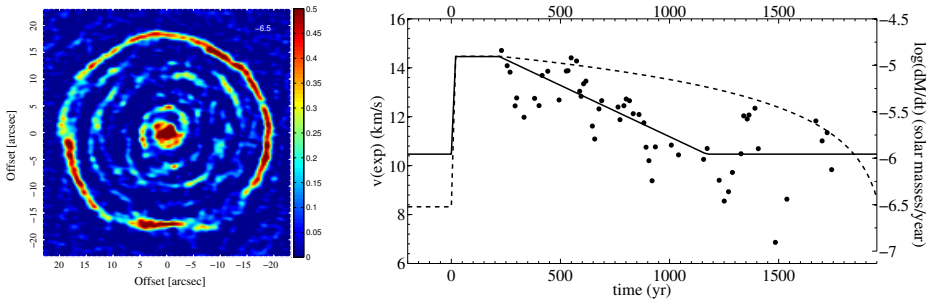

Figure 4. CO(3 – 2) observations towards the carbon AGB star R Sculptoris (*left*). The colour scale is given in Jy/beam. The observations clearly show the detached shell at ≈20", as well as a spiral structure extending from the shell inwards to the present-day mass-loss. The shell was created during a thermal pulse ca. 1800 years ago. A previously unknown binary companion then shaped the post-pulse mass-loss into a spiral shape, allowing to measure the thermal pulse and post-pulse evolution of the expansion velocity and mass-loss rate (*right*) (from Maercker et al. 2012).

3.2. The Boomerang Nebula

The Boomerang Nebula, the coldest object in the universe, was observed in CO line emission and continuum emission during ALMA Cycle 0 in the end of 2011 (Sahai et al. 2013). The data were obtained in bands 3 (CO(1 – 0) and nearby continuum) and 6 (CO(2 – 1) and nearby continuum) in the compact configuration. Band 3 was observed in a 7-point mosaic using 15 and 18 antennas and a total on-source time of 2.21 hr, while band 6 was observed in a single pointing using 15 antennas in 6 minutes. The final images reached an rms of 2.5 mJy/beam at 6.25 km/s resolution in the CO(1 – 0) line and an rms of 7.5 mJy/beam at 0.63 km/s resolution in the CO(2 – 1) map. Finally, the CO(1 – 0) map was combined with a single-dish SEST map at 8 km/s resolution to recover the extended flux.

The observations show that the biconical outflow that is seen in HST images traces hollow cavities in the cold, high-velocity outflow, with walls of high-density molecular gas and dust (Fig. 5). The expanding hourglass-shaped structure has a dense waist containing dust grains of several millimetres in size, with a total dust mass of ≈0.07 solar masses. The bipolar nebula is likely due to a fast jet interacting with the inner regions of the extremely cold outflow, and carving out biconical cavities in the central dusty structure. This will allow starlight to preferentially stream out in these directions, producing the bipolar appearance of the Boomerang Nebula in the *HST* images.

3.3. Shaping the outflow of binary AGB stars

High-angular resolution observations reveal the complex structures that are created through binary interaction with the winds from AGB stars. The incredible degree of complexity is apparent in ALMA images of CO(3 – 2) line emission towards the binary star system Mira AB (Ramstedt et al. 2014). In the ALMA data, several different dynamical actors are identified, leading to a number of morphological components in the images. The observations were taken with 30 antennas in the main array, as well as 7 antennas in the ACA. The total on-source observing times are 6.25 min and 6 min for the main array and ACA, respectively. The maximum recoverable scale in the main

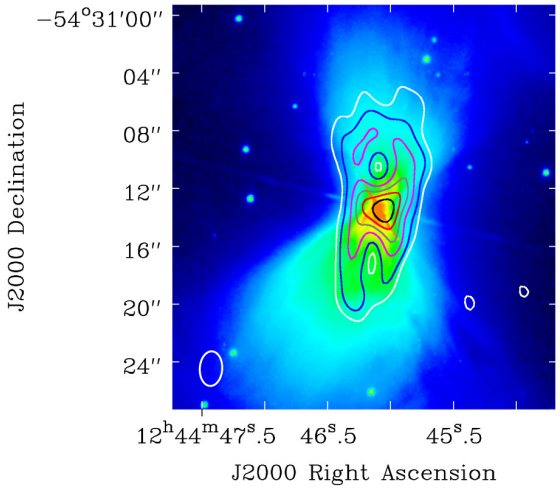

Figure 5. CO(2 − 1) observations towards the pre-planetary nebula The Boomerang Nebula at the systemic velocity (contours) overlaid on a false-color *HST* image taken with the F606W filter. The contour levels are at 37.5, 75, 150, 225, 300, and 375 mJy/beam. The rms in the ALMA contours is 7.5 mJy/beam. The beam is shown as the white ellipse in the lower left corner (from Sahai et al. 2013).

array observations is 6". Adding the observations from the ACA extends this scale to 9". The final images have an rms of 23 mJy/beam at ≈0.85 km/s resolution.

The binary companion is marginally resolved, and spiral arcs around the AGB star Mira A are found at the stellar velocity. In addition, the accretion wake is clearly visible behind the binary companion. Finally, there are signs of the fast wind of Mira B blowing a bubble in the expanding envelope of Mira A (Fig. 6). These are the most detailed observations of the molecular gas around Mira AB to date, and they reveal a complex interaction between binary stars and their winds that will challenge current hydrodynamical models. For more information on ALMA observations of binary AGB stars, see the contribution by S. Ramstedt in these proceedings.

4. Conclusions

Already in the first cycles of operation, ALMA has contributed significantly to our understanding of evolved stars. In fact, current models do not always manage to reproduce the complexity observed in the ALMA data. In order to fully describe the new data, it will be necessary to update hydrodynamical, radiative transfer, and chemical models. It is clear that at least some of these will need to be done in three dimensions, pushing current computing capabilities to their limit. The unique data produced by ALMA will mean a significant step forward in the field of evolved stars research, and can be used to demonstrate the importance of evolved stars as contributors to galaxy evolution not only to the scientific community, but also to public audiences.

Acknowledgments. MM acknowledges funding from the People Programme (Marie Curie Actions) of the European Union's Seventh Framework Programme (FP7/2007-2013) under REA grant agreement No. 623898.11.

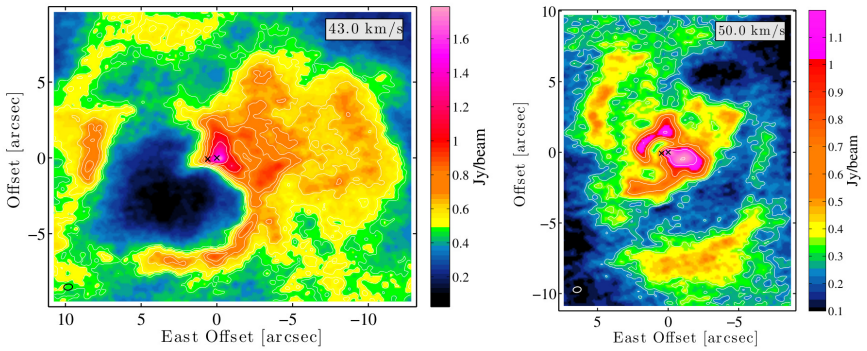

Figure 6. CO(3 − 2) observations with ALMA towards the Mira AB system averaged over 2 and 3 km/s around 43.0 km/s and 50km/s, respectively. The map on the left shows the bubble structure blown into the wind of Mira A by the companion Mira B. The map on the right shows spiral arcs created by the motion of the binary companion around Mira A (from Ramstedt et al. 2014).

References

Castro-Carrizo, A., Quintana-Lacaci, G., Neri, R., Bujarrabal, V., Schöier, F. L., Winters, J. M., Olofsson, H., Lindqvist, M., Alcolea, J., Lucas, R., & Grewing, M. 2010, A&A, 523, A59

Cernicharo, J., Daniel, F., Castro-Carrizo, A., Agundez, M., Marcelino, N., Joblin, C., Goicoechea, J. R., & Guélin, M. 2013, ApJ, 778, L25. 1310.7383

De Beck, E., Decin, L., de Koter, A., Justtanont, K., Verhoelst, T., Kemper, F., & Menten, K. M. 2010, A&A, 523. 1008.1083

De Beck, E., Kamiński, T., Patel, N. A., Young, K. H., Gottlieb, C. A., Menten, K. M., & Decin, L. 2013, A&A, 558, A132. 1309.5202

De Beck, E., Lombaert, R., Agúndez, M., Daniel, F., Decin, L., Cernicharo, J., Müller, H. S. P., Min, M., Royer, P., Vandenbussche, B., de Koter, A., Waters, L. B. F. M., Groenewegen, M. A. T., Barlow, M. J., Guélin, M., Kahane, C., Pearson, J. C., Encrenaz, P., Szczerba, R., & Schmidt, M. R. 2012, A&A, 539, A108. 1201.1850

Decin, L., Agúndez, M., Barlow, M. J., Daniel, F., Cernicharo, J., Lombaert, R., De Beck, E., Royer, P., Vandenbussche, B., Wesson, R., Polehampton, E. T., Blommaert, J. A. D. L., De Meester, W., Exter, K., Feuchtgruber, H., Gear, W. K., Gomez, H. L., Groenewegen, M. A. T., Guélin, M., Hargrave, P. C., Huygen, R., Imhof, P., Ivison, R. J., Jean, C., Kahane, C., Kerschbaum, F., Leeks, S. J., Lim, T., Matsuura, M., Olofsson, G., Posch, T., Regibo, S., Savini, G., Sibthorpe, B., Swinyard, B. M., Yates, J. A., & Waelkens, C. 2010, Nature, 467, 64. 1104.2316

González Delgado, D., Olofsson, H., Kerschbaum, F., Schöier, F. L., Lindqvist, M., & Groenewegen, M. A. T. 2003a, A&A, 411, 123. arXiv:astro-ph/0302179

González Delgado, D., Olofsson, H., Schwarz, H. E., Eriksson, K., & Gustafsson, B. 2001, A&A, 372, 885. arXiv:astro-ph/0104140

González Delgado, D., Olofsson, H., Schwarz, H. E., Eriksson, K., Gustafsson, B., & Gledhill, T. 2003b, A&A, 399, 1021

Justtanont, K., Khouri, T., Maercker, M., Alcolea, J., Decin, L., Olofsson, H., Schöier, F. L., Bujarrabal, V., Marston, A. P., Teyssier, D., Cernicharo, J., Dominik, C., de Koter, A., Melnick, G., Menten, K. M., Neufeld, D., Planesas, P., Schmidt, M., Szczerba, R., & Waters, R. 2012, A&A, 537, A144. 1111.5156

Khouri, T., de Koter, A., Decin, L., Waters, L. B. F. M., Lombaert, R., Royer, P., Swinyard, B., Barlow, M. J., Alcolea, J., Blommaert, J. A. D. L., Bujarrabal, V., Cernicharo, J.,

Groenewegen, M. A. T., Justtanont, K., Kerschbaum, F., Maercker, M., Marston, A., Matsuura, M., Melnick, G., Menten, K. M., Olofsson, H., Planesas, P., Polehampton, E., Posch, T., Schmidt, M., Szczerba, R., Vandenbussche, B., & Yates, J. 2014a, A&A, 561, A5. 1403.2892

Khouri, T., de Koter, A., Decin, L., Waters, L. B. F. M., Maercker, M., Lombaert, R., Alcolea, J., Blommaert, J. A. D. L., Bujarrabal, V., Groenewegen, M. A. T., Justtanont, K., Kerschbaum, F., Matsuura, M., Menten, K. M., Olofsson, H., Planesas, P., Royer, P., Schmidt, M. R., Szczerba, R., Teyssier, D., & Yates, J. 2014b, A&A, 570, A67. 1409.0396

Maercker, M., Mohamed, S., Vlemmings, W. H. T., Ramstedt, S., Groenewegen, M. A. T., Humphreys, E., Kerschbaum, F., Lindqvist, M., Olofsson, H., Paladini, C., Wittkowski, M., de Gregorio-Monsalvo, I., & Nyman, L.-A. 2012, Nature, 490, 232. 1210.3030

Maercker, M., Ramstedt, S., Leal-Ferreira, M. L., Olofsson, G., & Floren, H. G. 2014, A&A, 570, A101. 1409.4410

Maercker, M., Schöier, F. L., Olofsson, H., Bergman, P., Frisk, U., . Hjalmarson, Å., Justtanont, K., Kwok, S., Larsson, B., Olberg, M., & Sandqvist, A. 2009, A&A, 494, 243. 0812.1338

Maercker, M., Schöier, F. L., Olofsson, H., Bergman, P., & Ramstedt, S. 2008, A&A, 479, 779. arXiv:0801.0971

Olofsson, H., Maercker, M., Eriksson, K., Gustafsson, B., & Schöier, F. 2010, A&A, 515, A27+. 1003.0362

Ramstedt, S., Mohamed, S., Vlemmings, W. H. T., Maercker, M., Montez, R., Baudry, A., De Beck, E., Lindqvist, M., Olofsson, H., Humphreys, E. M. L., Jorissen, A., Kerschbaum, F., Mayer, A., Wittkowski, M., Cox, N. L. J., Lagadec, E., Leal-Ferreira, M. L., Paladini, C., Pérez-Sánchez, A., & Sacuto, S. 2014, A&A, 570, L14. 1410.1529

Ramstedt, S., Schöier, F. L., Olofsson, H., & Lundgren, A. A. 2008, A&A, 487, 645. 0806.0517

Richichi, A., Percheron, I., & Khristoforova, M. 2005, A&A, 431, 773

Sahai, R., Vlemmings, W. H. T., Huggins, P. J., Nyman, L.-Å., & Gonidakis, I. 2013, ApJ, 777, 92. 1308.4360

Schöier, F. L., Bast, J., Olofsson, H., & Lindqvist, M. 2007, A&A, 473, 871. arXiv:0707.0944

Schöier, F. L., Ryde, N., & Olofsson, H. 2002, A&A, 391, 577. arXiv:astro-ph/0206078